MOLECULAR AND CELLULAR BIOLOGY, Jan. 1995, p. 488–496 Vol. 15, No. 1
0270-7306/95/$04.00+0

Lack of an Effect of the Efficiency of RNA 3′-End Formation on the Efficiency of Removal of Either the Final or the Penultimate Intron in Intact Cells

DOBRILA NESIC,† JING ZHANG, AND LYNNE E. MAQUAT*

Department of Human Genetics, Roswell Park Cancer Institute, Buffalo, New York 14263

Received 15 June 1994/Returned for modification 8 August 1994/Accepted 28 September 1994

Evidence exists from studies using intact cells that intron removal can be influenced by the reactivity of upstream and downstream splice sites and that cleavage and polyadenylation can be influenced by the reactivity of upstream splice sites. These results indicate that sequences within 3′-terminal introns can function in the removal of upstream introns as well as the formation of RNA 3′ ends. Evidence from studies using intact cells for an influence of RNA 3′-end formation on intron removal is lacking. We report here that mutations within polyadenylation sequences that either decrease or increase the efficiency of RNA 3′-end formation have no effect on the efficiencies with which either the 3′-terminal or the penultimate intron is removed by splicing. Northern (RNA) blot hybridization, RNase mapping, and an assay that couples reverse transcription and PCR were used to analyze the effects of deletions and a substitution of the polyadenylation sequences within the human gene for triosephosphate isomerase (TPI). TPI pre-mRNA harbors six introns that are constitutively removed by splicing. Relative to normal levels, each of the deletions was found to reduce the nuclear and cytoplasmic levels of TPI mRNA, increase the nuclear level of unprocessed RNA 3′ ends, and decrease the nuclear level of processed RNA 3′ ends. In contrast, the substitution using the polyadenylation sequences of the mouse β^{major}-globin gene was found to increase the nuclear and cytoplasmic levels of TPI mRNA, decrease the nuclear level of unprocessed 3′ ends, and increase the nuclear level of processed 3′ ends. The simplest interpretation of these data indicates that (i) the rate of 3′-end formation normally limits the amount of mRNA produced and (ii) the deletions decrease and the substitution increases the efficiency of RNA 3′-end formation. While each of the deletions and the substitution altered the absolute levels of intron 6-containing, intron 5-containing, intron 6-free, and intron 5-free RNAs, in no case was there an abnormal ratio of intron-containing to intron-free RNA for either intron. Therefore, at least for TPI RNA, while the efficiency of removal of the 3′-terminal intron influences the efficiency of RNA 3′-end formation, the efficiency of RNA 3′-end formation does not influence the efficiency of removal of either the 3′-terminal or penultimate intron. The dependence of TPI RNA 3′-end formation on splicing may reflect the suboptimal strengths of the corresponding regulatory sequences and may function to ensure that TPI pre-mRNA is not released from the chromatin template until it has formed a complex with spliceosomes. If so, then the independence of TPI RNA splicing on 3′-end formation may be rationalized by the lack of a comparable function.

Most vertebrate pre-mRNAs are processed via steps in the nucleus that include capping at the 5′ end (39), polyadenylation at the 3′ end (43), and splicing to remove introns (11, 13, 31, 44). The mechanism of polyadenylation, which involves an endonucleolytic cleavage and the subsequent addition of 50 to 250 adenosine residues to the 3′ end of the proximal cleavage product, is directed by conserved RNA sequences that reside both upstream and downstream of the cleavage site as well as proteins that bind either directly or indirectly to the RNA sequences. The mechanism of splicing, which involves transesterification reactions of phosphodiester bond breakage and re-formation, is directed largely by conserved sequences at the 5′ and 3′ ends of the introns that interact either directly or indirectly with small ribonucleoproteins (RNPs) as well as a multitude of protein factors. Despite the finding that RNA 3′-end formation and splicing can proceed independently of one another in cell extracts (19, 29, 30), evidence indicates that the two processes are likely to be coupled in intact cells. It is generally accepted that the efficiency of RNA 3′-end formation is augmented by the 3′ splice site of the 3′-terminal intron (7, 14, 24, 28, 32, 36–38, 42, 45). In fact, it has even been suggested that polyadenylation site selection cannot take place in intact cells after intron excision (23). The idea that the efficiency of RNA 3′-end formation is augmented by the 3′ splice site of the 3′-terminal intron was corroborated and clarified by the finding that it is not the 3′ splice site per se but the efficiency with which the 3′-terminal intron is removed that dictates the efficiency of RNA 3′-end formation, at least for pre-mRNAs having suboptimal sequences that mediate each process (33). Whether for intact cells the converse is also true, i.e., whether sequences that direct RNA 3′-end formation can influence the efficiency with which the 3′-terminal intron is removed, is unknown. Evidence for such an influence derives from experiments using nuclear extracts and chimeric pre-mRNAs consisting of either one, two, or three introns from the adenovirus major late transcript fused upstream of sequences required for polyadenylation of the simian virus 40 (SV40) late transcript (36). In these experiments, functional inactivation of the AAUAAA element was found to impair removal of the 3′-terminal intron but have no effect on removal of the intron(s) that reside upstream of the 3′-terminal intron.

* Corresponding author. Mailing address: Department of Human Genetics, Roswell Park Cancer Institute, Elm and Carlton Sts., Buffalo, NY 14263. Phone: (716) 845-3325. Fax: (716) 845-8449. Electronic mail address: maquat@SC3101.med.buffalo.edu.

† Present address: Département de Biologie Cellulaire, Université de Genève, CH-1211 Geneva 4, Switzerland.

The aim of this study was to test if RNA 3′-end formation plays a role in splicing. The well-characterized pre-mRNA for the human glycolytic enzyme triosephosphate isomerase (TPI) was analyzed. Pre-mRNA was generated in mouse L cells by the transient expression of TPI genes in which the TPI promoter had been replaced by the mouse metallothionein-1 (MT-1) promoter. The genes harbored (i) deletions of the two strongest TPI polyadenylation hexanucleotide signals, (ii) a deletion that encompassed all TPI polyadenylation sequences, or (iii) a substitution of all TPI polyadenylation sequences with the mouse β^{major}-globin polyadenylation sequence (9), which is more efficient in polyadenylation than the combined TPI sequences. The coexpression of a reference globin (Gl) gene that was also driven by the MT-1 promoter was used to control for variations in the efficiencies of cell transfection and RNA recovery. Quantitations of the nuclear and cytoplasmic levels of MT-TPI mRNAs by Northern (RNA) blot hybridization, the nuclear levels of unprocessed and processed MT-TPI RNA 3′ ends by a sensitive RNase protection assay, and the nuclear levels of intron-containing and intron-free MT-TPI RNAs by an assay that couples reverse transcription (RT) and PCR indicated that the efficiencies with which the final and penultimate introns were removed by splicing were unaffected by variations in the efficiency of RNA 3′-end formation. Therefore, while the efficiency of final intron removal from TPI pre-mRNA influences the efficiency of TPI RNA 3′-end formation, the converse is not true.

MATERIALS AND METHODS

Cell culture, transfections, and RNA purification. The human melanoma cell line Malme-3 was grown in RPMI 1640 medium containing 10% bovine calf serum. Mouse Ltk$^-$ cells were grown in minimal essential medium containing 10% fetal calf serum and 5% bovine calf serum. Transfections were as described by Nesic et al. (32). Ltk$^-$ cells were transfected at 60 to 80% confluency with DEAE-dextran, a specific pMT-TPI test plasmid, and the pMT-Gl reference plasmid (12 μg of each per 15-cm-diameter dish). Nuclear and cytoplasmic RNAs were isolated 36 to 40 h after transfection.

Construction of pMT-TPI DNAs with abnormal polyadenylation signals. (i) Δ(pA1+pA2). The 659-bp *Eco*RI-*Nae*I fragment of the TPI gene that includes 477 bp of exon 7 and 182 bp of 3′ flanking DNA was subcloned into the *Eco*RI and Klenow-treated *Pst*I sites of M13mp18. The 6-nucleotide (nt) polyadenylation signals of the pA1 and pA2 sites were simultaneously deleted from the subclone by the method of Kunkel et al. (20) and the mutagenic oligonucleotides 5′ GACCTAGTGCCAGG(Δ)CCCTCACATGG 3′ and 5′ CTTGCACAAATG ATCA(Δ)TAGCTGCCTCAAAAGG 3′, where (Δ) denotes the deleted nucleotides. To reconstruct pMT-TPI DNA, the mutagenized fragment was sequenced in entirety and ligated to a 1-kbp *Nae*I-*Eco*RI fragment, which consists of human DNA sequences 3′ to the mutagenized fragment, and a 6.1-kbp *Eco*RI-*Eco*RI fragment, which consists of pUC13 DNA and TPI gene exons 1 through the distal part of exon 7.

(ii) Δ(*Nco*I-*Nae*I). A 1.6-kbp *Eco*RI-*Eco*RI fragment of the TPI gene that includes 475 bp of exon 7 and 1.12 kbp of 3′ flanking DNA was subcloned into pUC13 DNA. The plasmid was then cleaved with *Nco*I and *Nae*I and subsequently recircularized to remove 63 bp of the 3′ untranslated region and 182 bp of 3′ flanking DNA, i.e., all known sequences that direct RNA 3′-end formation. Regeneration of the *Nco*I site upon recircularization and DNA sequencing were used to assess the integrity of the deletion product prior to reconstructing the pMT-TPI derivative. Reconstruction of pMT-TPI DNA involved ligation of the mutagenized 1.6-kbp *Eco*RI-*Eco*RI fragment to the 6.1-kbp *Eco*RI-*Eco*RI fragment.

(iii) Δ(*Nco*I-*Nae*I)/β-Gl. A 138-bp *Pvu*II-*Hin*cII fragment that spans the mouse β^{major}-globin polyadenylation sequences (9) and includes 68 bp of exon 3 and 70 bp of 3′ flanking DNA was generated by PCR using the primers 5′ CTGTCAG CTGTTGGCAAAATG3′ and 5′ GACCTGAACGTTGACTTCTTTGTATC 3′, where the underlined sequences denote the *Pvu*II and *Hin*cII sites, respectively. The resulting PCR product was cleaved with *Pvu*II and *Hin*cII and subsequently inserted into the regenerated *Nco*I site of the 1.6-kbp *Eco*RI-*Eco*RI subclone (see above) that had been cleaved and made blunt ended by using Klenow enzyme and deoxynucleoside triphosphates. pMT-TPI DNA was reconstructed as described for the Δ(*Nco*I-*Nae*I) construct.

RNA blotting. Nuclear and cytoplasmic RNAs (25 μg) were denatured, electrophoresed, transferred to nylon (Zeta-bind), and hybridized to ^{32}P-labeled DNA fragments as previously described (32). MT-TPI RNA was detected with a 300-bp *Nco*I-*Nde*I fragment that derived from the 3′ untranslated region of human TPI cDNA. MT-Gl RNA was detected with a mixture of 170-bp *Msc*I-*Dra*I fragment that derived from exon 3 of the mouse β^{major}-mouse globin gene and a 427-bp *Nhe*I-*Eco*RI fragment that includes 417 bp of exons 1 through 3 of human β-globin cDNA plus sequences from pSP64 DNA. Hybridization and washing conditions were such that human but not mouse TPI RNA was detected (4). Quantitative analysis was performed with a PhosphorImager (Molecular Dynamics).

RNase mapping. Uniformly ^{32}P-labeled antisense RNA probes for the mapping of TPI and β-globin transcripts were synthesized from linearized pGEM vectors by using T7 RNA polymerase (Promega) as described previously (32). Antisense RNA to the 642-bp *Nde*I-*Pvu*II fragment of the TPI gene, which includes 365 bp of the 3′ untranslated region and 277 bp of 3′ flanking DNA, or to either deletion or substitution derivatives of this fragment was used to map the cleavage and polyadenylation sites of TPI RNA. Deletion derivatives consisted of the 630-bp fragment that harbored deletions of the two polyadenylation signals or the 397-bp fragment that harbored the *Nco*I-*Nae*I deletion. The substitution derivative consisted of the 535-bp *Nde*I-*Pvu*II fragment that harbored the 138-bp *Pvu*II-*Hin*cII fragment inserted at the junction of the *Nco*I-*Nae*I deletion. Antisense RNA to the 235-bp *Bam*HI-*Mbo*II fragment from mouse β^{major}-globin cDNA, which includes 19 bp of exon 2 and 216 bp of exon 3, was used to control for experimental variations. The resulting transcripts were used to analyze either L-cell or Malme-3 cell RNA by RNase mapping as previously described (32). Quantitative analysis was performed with a PhosphorImager.

RT-PCR analyses. The RT-PCR analyses were essentially as described previously (33) except that for each PCR sample, 6 μl of the 20-μl RT reaction was brought to 50 μl so as to contain 140 μM each of the four deoxynucleoside triphosphates, 100 pmol of each of the sets of primers, and 3.25 U of *Taq* DNA polymerase (Promega). After 19 amplification cycles, 1/10 of the PCR mixture was electrophoresed in a 5 or 7% native polyacrylamide gel, and the PCR products were quantitated by PhosphorImager analysis.

PCR primer pairs. TPI cDNA primers amplified exon 5-exon 6 (5′ AGACTGCAACACCCCAAC 3′ [sense]; 5′ AGCCACCGCATCAGAGCGT TGGACTTCAGCCA 3′ [antisense]; PCR product with intron 5, 354 bp; PCR product without intron 5, 83 bp) or exon 6-exon 7 (5′ GAAGTCCAACGTCTCT 3′ [sense]; 5′ AATTCGGGCTTGAGGGAAG 3′ [antisense]; PCR product with intron 6, 276 bp; PCR product without intron 6, 150 bp). The β-globin cDNA primers amplified intron 1-exon 2 (5′ GCCTATTGGTCTATTTTCCC 3′ [sense]; 5′ CCTGAAGTTCTCAGGATCC 3′ [antisense]; PCR product, 250 bp).

RESULTS

The level of TPI mRNA production varies as a function of the polyadenylation sequence(s). It was shown previously that the efficiency with which the last intron of TPI pre-mRNA is removed by splicing influences the efficiency of TPI pre-mRNA 3′-end formation (33). To determine if the converse is also true, i.e., if the efficiency of TPI pre-mRNA 3′-end formation influences the efficiency of final intron removal, the multiple polyadenylation sequences of the TPI gene were partially deleted, almost entirely deleted, or substituted with a stronger polyadenylation sequence. Initially, the major (AATAAA) and minor (TATAAA) polyadenylation signals, which reside 83 nt apart and are referred to as pA1 and pA2, respectively (33), were deleted to create the pMT-TPI derivative called Δ(pA1+pA2) (Fig. 1). Subsequently, the 242-bp region that extends from the *Nco*I site in exon 7 to the *Nae*I site in 3′ flanking DNA and includes 65 bp of the 3′ untranslated region and 177 nt of 3′ flanking DNA (i.e., 113 nt downstream of the pA2 site) was deleted to create the pMT-TPI derivative called Δ(*Nco*I-*Nae*I) (Fig. 1). Finally, the region that was missing from Δ(*Nco*I-*Nae*I) was replaced with a 138-bp *Pvu*II-*Hin*cII fragment that includes the single polyadenylation sequence of the mouse β^{major}-globin gene (9) to create the pMT-TPI derivative called Δ(*Nco*I-*Nae*I)/β-Gl (Fig. 1).

Each pMT-TPI plasmid was transiently expressed in mouse L cells together with the reference pMT-Gl plasmid. The level of each product mRNA was quantitated by Northern blot hybridization. Deletion of the pA1 and pA2 sites increased the size of nuclear and cytoplasmic MT-TPI mRNAs by about 112 nt and reduced the level of the mRNAs to 24 and 29% of normal, respectively (Fig. 2). These results indicate that additional sites of RNA cleavage and polyadenylation are used, at least in the absence of the hexanucleotide signals of the two

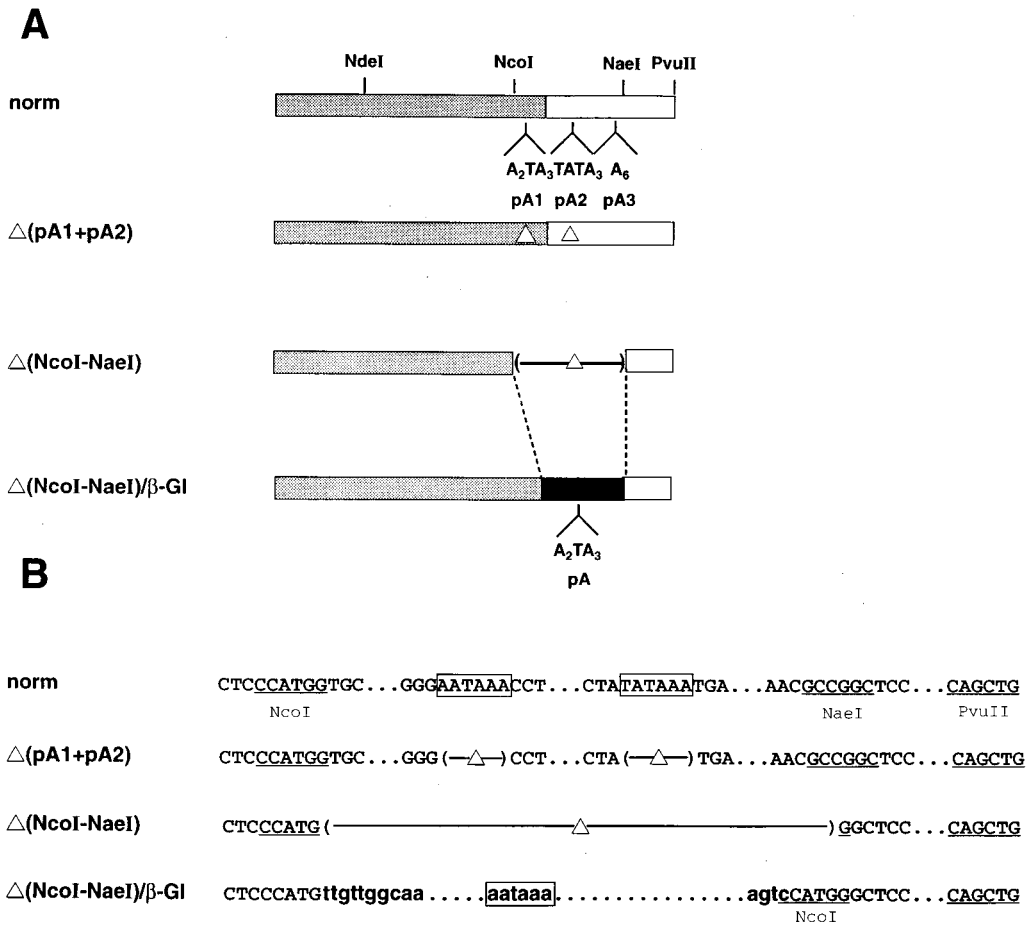

FIG. 1. Structures and sequences of the pMT-TPI constructs that harbor deletions or a substitution of the polyadenylation sequences. (A) Diagram of the last exon and 3′ flanking DNA of the normal pMT-TPI construct and its derivatives. Hatched boxes represent all (565 bp) of exon 7, open boxes represent 3′ flanking DNA, and the solid box represents the mouse β^{major}-globin polyadenylation sequence. The position and nucleotide composition of the hexanucleotide signals of each putative polyadenylation site (pA) are provided. The β-globin polyadenylation site is not numbered since it is unique, whereas the putative TPI sites are sequentially numbered. Δ denotes deletion of either the pA1 (AATAAA) and pA2 (TATAAA) hexanucleotide signals or the 245-bp *Nco*I-*Nae*I fragment. Vertical dotted lines from the *Nco*I-*Nae*I deletion to the β-globin insertion indicate that the insertion was substituted for the deleted sequences. (B) Sense-strand sequences of the normal pMT-TPI construct and its derivatives. Boxes denote the pA1 and pA2 hexanucleotide signals of the TPI gene and the pA hexanucleotide of the β^{major}-globin gene. Δ denotes deletion, and dots denote sequences present in the construct but not shown. From left to right, the dots specify 38, 66, 86, and 105 nt for the normal (norm) and Δ(pA1+pA2) constructs and 33, 85, and 86 nt for the Δ(*Nco*I-*Nae*I)/β-Gl construct. Lowercase letters in boldface represent 138 bp of mouse β^{major}-globin DNA that are required for efficient cleavage and polyadenylation (9). *Nco*I, *Nae*I, and *Pvu*II sites are specified for the normal construct and underlined for the derivatives.

major sites (Fig. 2). In fact, hints that at least one site of RNA cleavage and polyadenylation residing downstream of the pA2 site is normally used, albeit with barely detectable efficiency, derive from the analysis using RNase mapping of either pMT-TPI transcripts or TPI RNA of the human melanoma cell line of Malme-3 (32, 33) (see below). The *Nco*I-*Nae*I deletion removed not only the pA1 and pA2 sites but also the minor downstream site(s) and, consistent with this observation, reduced the nuclear and cytoplasmic levels of MT-TPI mRNA to less than 1% of normal. Insertion of the single mouse β^{major}-globin polyadenylation sequence at the junction of the *Nco*I-*Nae*I deletion restored the sizes of nuclear and cytoplasmic MT-TPI mRNAs to approximately normal, as expected given that the transcribed portion of the mRNA is predicted to be only 5 nt larger than that of the normal MT-TPI mRNA (18, 26), and increased the levels of the mRNAs to 154 and 200% of normal, respectively. The simplest interpretation of these results is the one predicted from previous studies of mouse β^{major}-globin RNA 3′-end formation (9); i.e., the mouse β^{major}-globin polyadenylation sequence is more effective than the sum of the TPI polyadenylation sequences in directing the amounts of nascent transcripts that are processed to mRNA. It is possible that the deletion and the substitution of the polyadenylation sequences, respectively, destabilize and stabilize nuclear MT-TPI RNA apart from or as a consequence of affecting RNA 3′-end formation. However, any effects of the mutations on nuclear mRNA half-life abundance appear to be primarily the result of effects on the efficiency of RNA 3′-end formation (see below). None of the mutations, with the possible exception of the Δ(*Nco*I-*Nae*I)/β-Gl mutations (see below), appears to alter the half-life of cytoplasmic mRNA, since all but the Δ(*Nco*I-*Nae*I)/β-Gl mutation is associated with a level of cytoplasmic mRNA that is comparable to the level of nuclear mRNA when the levels are expressed as percentages of normal (Fig. 2).

The efficiency of TPI RNA 3′-end formation can be increased or decreased depending upon the strength of the polyadenylation sequence. The Northern blot data suggested that mutation of the TPI polyadenylation sequences alters the level of product mRNA because of changes in the efficiency and,

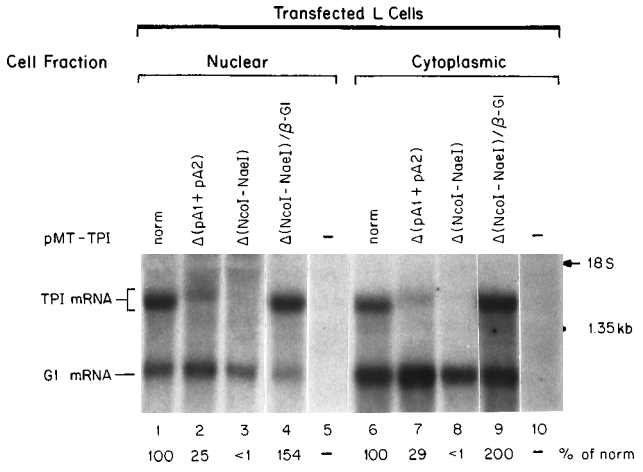

FIG. 2. The abundance of MT-TPI mRNA varies depending upon the polyadenylation sequence. Mouse L cells were cotransfected with 12 μg of the specific pMT-TPI construct and 12 μg of reference pMT-Gl DNA. Nuclear and cytoplasmic RNAs (25 μg) from transfected and untransfected L cells were denatured, electrophoresed in agarose, transferred to a nylon membrane, and cohybridized with the ^{32}P-labeled 300-bp *Nde*I-*Nco*I fragment of the human TPI gene, the ^{32}P-labeled 427-bp *Nhe*I-*Eco*RI of human β-globin cDNA, and the ^{32}P-labeled 170-bp *Msc*I-*Dra*I fragment of the mouse β^{major}-globin gene. The level of each MT-TPI RNA was normalized to the level of MT-Gl RNA and then calculated as a percentage of normal (norm) MT-TPI mRNA, which was defined as 100%. Numbers represent the averages of five independently performed experiments. The values for percentage of normal differed between the experiments using Δ(pA1+pA2), Δ(*Nco*I-*Nae*I), and Δ(*Nco*I-*Nae*I)/β-gl by ≤6%, undetectably, and by ≤19%, respectively. mRNA that derives from the Δ(pA1+pA2) construct is abnormally large as a result of utilization of the one or more of the minor downstream cleavage and polyadenylation sites (see text). The electrophoretic positions of 18S RNA and a 1.35-kb RNA standard are indicated.

possibly, position(s) of RNA 3′-end formation. To analyze this possibility further, the effects of the deletions and substitution on RNA 3′-end formation were analyzed directly, using RNase mapping and uniformly ^{32}P-labeled antisense RNAs as probes (32, 33). The 3′ ends of TPI transcripts that derived from one of the MT-TPI constructs or the endogenous TPI gene of Malme-3 cells were localized and quantitated by using probes that extended from the *Nde*I site within the 3′ untranslated region of exon 7 to the *Pvu*II site within 3′ flanking DNA. The probe also included sequences from the pGEM expression vector at each end. Since it was important to maintain colinearity between the probe and each MT-TPI transcript under analysis, different probes were used to map different transcripts. Therefore, the probes had identical endpoints but varied in size in order to harbor the deletion or substitution of the transcript under analysis. The endpoints extended from the *Nde*I site within exon 7 of the TPI gene to the *Pvu*II site within 3′ flanking DNA (Fig. 3). The probe for the normal MT-TPI transcripts consisted of 699 nt, 642 of which derived from TPI gene sequences and included 365 nt of the 3′ untranslated region and 277 nt of 3′ flanking DNA (32, 33). The probe for the Δ(pA1+pA2) transcripts consisted of 687 nt, 630 of which derived from TPI gene sequences and included 359 nt of the 3′ untranslated region and 271 nt of 3′ flanking DNA. The probe for the Δ(*Nco*I-*Nae*I) transcripts consisted of 454 nt, 397 of which derived from TPI gene sequences and included 299 nt of the 3′ untranslated region and 98 nt of 3′ flanking DNA. The probe for the Δ(*Nco*I-*Nae*I)/β-Gl transcripts consisted of 592 nt, 535 of which derived from the hybrid TPI-Gl gene and consisted of 299 nt of TPI 3′ untranslated region, 68 nt of the mouse β^{major}-globin gene 3′ untranslated region, 70 nt of the mouse β^{major}-globin gene 3′ flanking DNA, and 98 nt of TPI 3′ flanking DNA. The MT-Gl reference transcripts were mapped by using a probe of 298 nt, 235 of which derived from mouse β^{major}-globin cDNA and included 19 nt of exon 2 and 216 nt of exon 3 (32, 33). Protected fragments of each probe were quantitated by radiographic imaging, and imaging intensities were corrected for the number of radioactive nucleotides. Subsequently, the quantity of each fragment was normalized to the quantity of the reference globin fragment and then calculated as a percentage of the value for the corresponding normal MT-TPI transcript, which was invariably defined as 100.

RNA from the normal MT-TPI construct, like RNA from the endogenous gene of Malme-3 cells, protected several regions of the TPI probe from RNase digestion. The most abundant protected fragment that was detected with both nuclear and cytoplasmic RNAs migrated at 365 nt (Fig. 3A, lanes 1, 2, 11, and 12) and was the result of hybridization to MT-TPI RNA or human TPI RNA that had been cleaved (C^+) and polyadenylated (A^+) at the major polyadenylation site, pA1 (32, 33). This RNA will be referred to as C_1^+/A_1^+. Other protected fragments of the TPI probe migrated at approximately 642 and 446 nt (Fig. 3A, lanes 1, 2, 11, and 12). The 642-nt fragment was the result of hybridization to transcripts having 3′ ends that extended beyond the limits of the probe and were neither cleaved nor polyadenylated (C^-/A^- RNA). The 446-nt fragment that was detected with nuclear RNA resulted from hybridization to a mixture of transcripts, some of which had been cleaved and polyadenylated at the minor pA2 site (C_2^+/A_2^+ RNA) and some of which were C^-/A^- RNA generated during RNase mapping because of RNase cleavage within the stretch of 13 A residues that resides 83 nt downstream of the pA1 site (32, 33). The small amount of the 446-nt fragment that was detected with the cytoplasmic RNA of Malme-3 cells is likely to be the result of hybridization to transcripts that are C_2^+/A_2^+ RNAs (32, 33). Additional protected fragments that were more readily detected with Malme-3 cell RNA than with MT-TPI RNA undoubtedly reflect the use of other minor sites of polyadenylation that reside either upstream (pA′) or downstream (pA3) of the pA2 site (32, 33) (Fig. 3A, lanes 11 and 12). Cleavage at the pA′ site, which according to sequence analysis actually consists of six sites that span a stretch of 8 nt, is thought to be dependent upon the AAUAAA hexanucleotide of the pA1 site (32) and may reflect mismatch of the TPI RNA cleavage site (GU) with the consensus cleavage site (CA) (41). Usage of the pA1, pA2, and pA3 sites is more or less in keeping with usage in vitro of pA sites having the same noncanonical hexanucleotide polyadenylation signals (40, 46).

RNA from the Δ(pA1+pA2) construct protected three regions of the probe from RNase digestion (Fig. 3A, lanes 3 and 4). The 630-nt fragment derived from hybridization to C^-/A^- RNA. The 450-nt fragment was likely to be the result of hybridization to transcripts that were cleaved and polyadenylated at the putative pA3 site (C_3^+/A_3^+ RNA), since the fragment comigrated with the pA3 fragment that was detected by using Malme-3 cell RNA (Fig. 3A, lanes 3, 4, 11, and 12). The 435-nt fragment was likely to be the result of hybridization to transcripts that were either C^-/A^- or C_3^+/A_3^+ but that had been digested by RNases during the protection assay within the stretch of 13 A residues. As expected, the 359-nt fragment was not detected in either cell fraction since deletion of the pA1 and pA2 hexanucleotide signals precluded usage of the pA1 and pA2 sites. Since only C^+/A^+ RNA is thought to be exported to the cytoplasm (8), the cytoplasmic levels of the 450- and 435-nt fragments may approximate the amount of nuclear C^+/A^+ RNA. However, the cytoplasmic levels could underestimate the amount of nuclear C^+/A^+ RNA since C^+/A^+ RNA

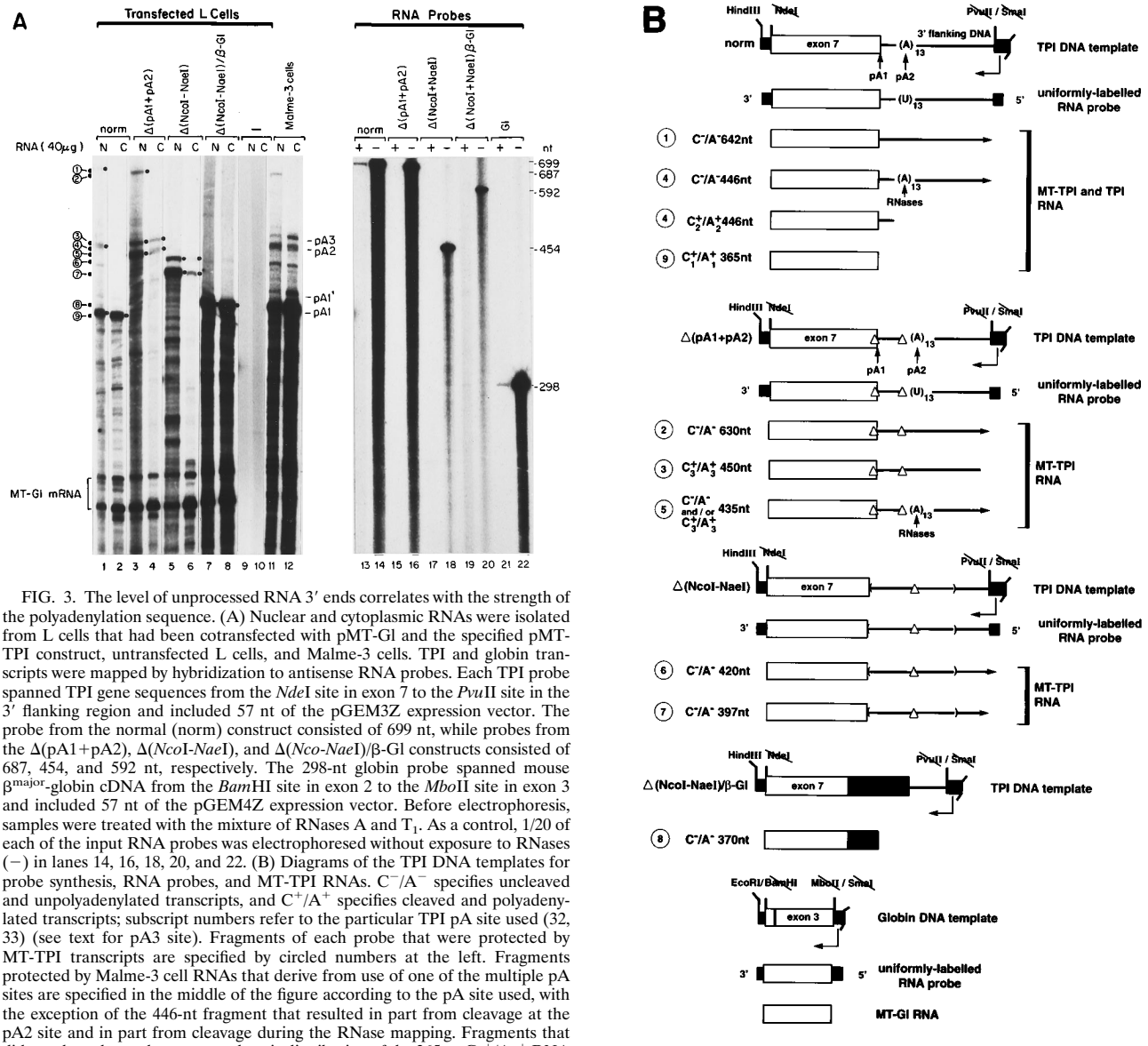

FIG. 3. The level of unprocessed RNA 3′ ends correlates with the strength of the polyadenylation sequence. (A) Nuclear and cytoplasmic RNAs were isolated from L cells that had been cotransfected with pMT-Gl and the specified pMT-TPI construct, untransfected L cells, and Malme-3 cells. TPI and globin transcripts were mapped by hybridization to antisense RNA probes. Each TPI probe spanned TPI gene sequences from the *Nde*I site in exon 7 to the *Pvu*II site in the 3′ flanking region and included 57 nt of the pGEM3Z expression vector. The probe from the normal (norm) construct consisted of 699 nt, while probes from the Δ(pA1+pA2), Δ(*Nco*I-*Nae*I), and Δ(*Nco*-*Nae*I)/β-Gl constructs consisted of 687, 454, and 592 nt, respectively. The 298-nt globin probe spanned mouse β^{major}-globin cDNA from the *Bam*HI site in exon 2 to the *Mbo*II site in exon 3 and included 57 nt of the pGEM4Z expression vector. Before electrophoresis, samples were treated with the mixture of RNases A and T_1. As a control, 1/20 of each of the input RNA probes was electrophoresed without exposure to RNases (−) in lanes 14, 16, 18, 20, and 22. (B) Diagrams of the TPI DNA templates for probe synthesis, RNA probes, and MT-TPI RNAs. C^-/A^- specifies uncleaved and unpolyadenylated transcripts, and C^+/A^+ specifies cleaved and polyadenylated transcripts; subscript numbers refer to the particular TPI pA site used (32, 33) (see text for pA3 site). Fragments of each probe that were protected by MT-TPI transcripts are specified by circled numbers at the left. Fragments protected by Malme-3 cell RNAs that derive from use of one of the multiple pA sites are specified in the middle of the figure according to the pA site used, with the exception of the 446-nt fragment that resulted in part from cleavage at the pA2 site and in part from cleavage during the RNase mapping. Fragments that did not show the nuclear-to-cytoplasmic distribution of the 365-nt C_1^+/A_1^+ RNA were not judged to derive from C^+/A^+ RNA. Transcripts from the normal MT-TPI construct protected fragments of 642, 446, and 365 nt and correspond, respectively, to C^-/A^- RNA, a mixture of C^-/A^- and C^+/A^+ RNA, and C_1^+/A_1^+ RNA. Transcripts from the Δ(pA1+pA2) construct protected fragments of 630, 450, and 435 nt and correspond, respectively, to C^-/A^-, C_3^+/A_3^+, and a mixture of C^-/A^- and C_3^+/A_3^+. Transcripts from the Δ(*Nco*I-*Nae*I) construct protected fragments of 420 and 397 nt. Both correspond to transcripts that extend beyond the 5′ end of the probe. The 420-nt fragment corresponds to the fraction of these transcripts that fortuitously protect sequences of the probe that may derive from pGEM DNA. Transcripts from the Δ(*Nco*I-*Nae*I)/β-Gl construct protected a fragment of 370 nt and correspond to C^+/A^+ RNA. Transcripts from the pMT-Gl construct protected fragments of 250 and 235 nt.

that is otherwise incompletely or improperly processed may be inhibited from export to the cytoplasm (21). These levels totaled 31% of the cytoplasmic level of C_1^+/A_1^+ RNA from the normal MT-TPI construct and were accompanied by a nuclear level of C^-/A^- RNA that was 220% of normal (Table 1). Therefore, consistent with the Northern blot data, deletion of the pA1 and pA2 sites reduces but does not preclude 3′-end formation. Notably, the finding that inefficiencies in RNA 3′-end formation result in the nuclear accumulation rather than the degradation of C^-/A^- RNA is consistent with earlier studies of mutations within intron sequences (32, 33).

RNA from the Δ(*Nco*I-*Nae*I) construct protected 420- and 397-nt regions of the probe (Fig. 3A, lanes 5 and 6). While the 397-nt fragment was the result of hybridization to transcripts that were C^-/A^-, protection of the larger fragment is difficult to explain since there is no appreciable complementarity between pGEM sequences of the probe and MT-TPI RNA that was transcribed from 3′ flanking DNA. Assuming that both fragments represent C^-/A^- RNA, the deletion increased the nuclear level of C^-/A^- RNA to approximately 640% of normal (Table 1). However, detection of each fragment in cytoplasmic RNA suggests that some of the transcripts might be C^+/A^+ RNAs. These RNAs constitute approximately 9% of the level of cytoplasmic C^+/A^+ RNA from the normal construct (Table 1) and are unlikely to be fully processed mRNA, as evidenced by the lack of detectable nuclear and cytoplasmic mRNAs from the Δ(*Nco*I-*Nae*I) construct by Northern blot hybridization (Fig. 2).

RNA from the Δ(*Nco*I-*Nae*I)/β-Gl construct protected a

TABLE 1. Cellular TPI RNA levels

TPI RNA	Nuclear RNA[a]				Cytoplasmic RNA (% of normal), C^+/A^+
	% of $[C^-/A^- + C^+/A^+]$		% of normal		
	C^-/A^-	C^+/A^+	C^-/A^-	C^+/A^+	
MT-TPI					
Normal	22 ± 6	78 ± 6	100	100	100
Δ(pA1+pA2)	NM	NM	220 ± 5	NM	31 ± 16
Δ(*Nco*I-*Nae*I)	NM	NM	640 ± 140	NM	9 ± 1
Δ(*Nco*I-*Nae*I)/β-Gl	0	100	0	114 ± 14	192 ± 6
TPI of Malme-3 cells	16 ± 2	84 ± 2	–	–	–

[a] NM, not measurable. The designation of C^+/A^+ RNA by NM derives from ambiguities in identifying those species that were, in fact, cleaved and polyadenylated in vivo. The designation of C^-/A^- by NM derives from a dependence of the calculation on C^+/A^+ RNA that proved to be NM.

single 370-nt region of the probe (Fig. 3A, lanes 7 and 8). This fragment was the result of hybridization to transcripts that had 3′ ends at the single cleavage and polyadenylation site of the mouse β^{major}-globin gene. Use of this site generates an RNA that is 5 nt longer than C^+/A^+ RNA from the normal MT-TPI construct. The lack of detectable C^-/A^- RNA and levels of nuclear and cytoplasmic C^+/A^+ RNAs that were, respectively, 114 and 192% of normal (Table 1) confirm the conclusion of the Northern blot data that β-globin sequences direct RNA 3′-end formation significantly more efficiently than TPI sequences. Consistent with the Northern blot analysis (Fig. 2), the higher level of C^+/A^+ RNA in cytoplasmic relative to nuclear RNA may reflect a stabilizing effect of the β-globin substitution on cytoplasmic mRNA.

A potential complication of the RNase mapping experiments is that some or all of the mutations result in the use of sites of RNA 3′-end formation that reside beyond the limits (i.e., downstream of) the probes used in RNase mapping so that the mapping products comigrate with C^-/A^- RNA. However, no such polyadenylated species were detected by Northern blot hybridization for any of the mutations (Fig. 2). Therefore, the simplest interpretation of the RNase mapping and RNA blot data is that the alterations in the polyadenylation sequences affect the efficiency of 3′-end formation.

The efficiency of TPI RNA 3′-end formation does not influence the efficiency of removal of the last two introns. The availability of a series of four MT-TPI constructs that manifested different efficiencies of RNA 3′ end formation and that had identical exon-intron configurations except at the 3′ terminus of the last exon allowed for an analysis of the issue at hand—whether the efficiency of RNA 3′-end formation influences the efficiency of splicing. Since the results of a previous study of MT-TPI transcripts indicated that the efficiency of final intron removal influenced the efficiency of RNA 3′ end formation (33), the nuclear levels of RNAs that did and did not contain the final intron, intron 6, were initially established for transcripts that derived from each of the MT-TPI constructs. The analysis coupled RT and PCR (5, 33) and is identical to the method that was previously used to demonstrate changes in the levels of intron-containing and intron-free RNA as a consequence of particular intron deletions (33). cDNA was made from nuclear RNA by using random hexamers. MT-TPI and MT-Gl cDNAs were subsequently amplified by using specific primer pairs. One primer pair amplified exon 6 through exon 7 of TPI RNA in a way that generated products of the same size for each of the MT-TPI constructs. The other primer pair amplified intron 1 through exon 2 of MT-Gl RNA. Conditions were empirically established to provide a linear relationship between the amount of each RT-PCR product and the amount of input RNA (Fig. 4). In agreement with previous findings (33), the products of MT-TPI RNAs as well as the TPI RNA of Malme-3 cells consisted of 276 and 151 bp and derived from intron 6-containing and intron 6-free RNAs, respectively (Fig. 4). The product of MT-Gl RNA consisted of 250 bp (Fig. 4). Each RT-PCR product was quantitated by radiographic imaging.

Normally, intron 6-containing and intron 6-free MT-TPI RNAs comprise, respectively, 14 and 86% of nuclear MT-TPI RNA in transfected L cells (Fig. 4; Table 2). Comparably, intron 6-containing and intron 6-free TPI RNAs comprise, respectively, 20 and 80% of nuclear TPI RNA in Malme-3 cells (Fig. 4; Table 2). While Δ(pA1+pA2) and Δ(*Nco*I-*Nae*I) constructs produced levels of intron 6-containing and intron 6-free RNAs that ranged from approximately 170 to 230% of normal, the relative percentages of the two RNAs remained essentially normal, i.e., approximately 14 and 86%, respectively (Fig. 4; Table 2). Therefore, a reduction in the efficiency of RNA 3′-end formation so that an abnormally high level of RNA remains tethered to the chromatin template results in an abnormal accumulation of both spliced and unspliced RNAs (see Discussion) but does not change the efficiency of intron 6 removal. The Δ(*Nco*I-*Nae*I)/β-Gl construct produced levels of

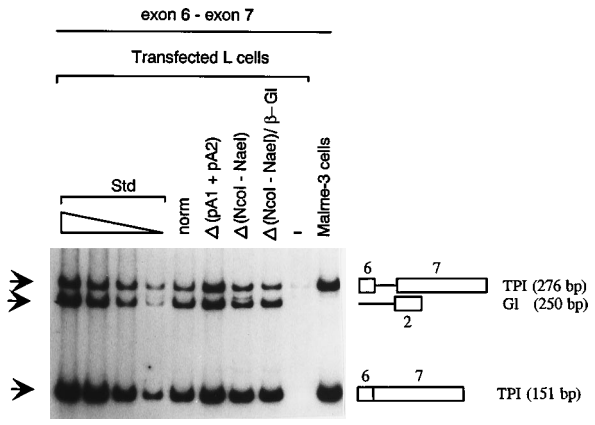

FIG. 4. The efficiency of TPI RNA 3′-end formation does not influence the efficiency with which the 3′-terminal intron, intron 6, is removed by splicing. Nuclear RNA (2.5 μg) from L cells that were transfected with pMT-Gl DNA and the designated pMT-TPI construct, untransfected L cells, or Malme-3 cells was amplified by RT-PCR. TPI RNA was amplified from exon 6 through exon 7. MT-Gl pre-mRNA was simultaneously amplified from intron 1 through exon 2 as a control. PCR products were electrophoresed in a 5% polyacrylamide gel and quantitated by PhosphorImager analysis. The conditions used for each RT-PCR were demonstrated to be quantitative by using RNA standards (Std) that consisted of serial dilutions (3, 1, 0.3, and 0.1 μg) of a nuclear RNA from transfected L cells. Structures and sites of the amplification products are shown at the right. norm, normal construct.

TABLE 2. Nuclear TPI RNA levels

TPI RNA	% of [(+int6[a]) + (−int6)]		% of normal	
	+int6	−int6	+int6	−int6
MT-TPI				
Normal	14 ± 3	86 ± 3	100	100
Δ(pA1+pA2)	17 ± 4	83 ± 4	185 ± 40	170 ± 30
Δ(*Nco*I-*Nae*I)	12 ± 3	88 ± 3	178 ± 30	232 ± 80
Δ(*Nco*I-*Nae*I)/β-Gl	17	83	98 ± 19	130 ± 8
TPI of Malme-3 cells	20 ± 7	80 ± 7		

[a] int6, intron 6.

intron 6-containing and intron 6-free MT-TPI RNAs that were on average 98 and 130% of normal, respectively, and also did not produce an appreciably altered ratio of the two RNAs (Fig. 4; Table 2). Therefore, alterations in the efficiency of RNA 3′-end formation because of changes within the polyadenylation sequences are inconsequential to the efficiency of intron 6 removal.

The results of a previous study of MT-TPI transcripts demonstrated that the deletion of intron 6 decreased the efficiency of intron 5 removal, suggesting that efficient removal of intron 5 is dependent on sequences within intron 6 (33). Since the removal of intron 6 is not affected by the process of RNA 3′-end formation, it is unlikely that the removal of intron 5 would be affected by the process of RNA 3′-end formation. For different reasons, this prediction is also supported by studies from the Berget laboratory of a chimeric pre-mRNA that consisted of either one, two, or three introns from the adenovirus major late transcript fused upstream of sequences that are required for polyadenylation of the SV40 late transcript (36). The studies demonstrated that mutation of the SV40 hexanucleotide signal impaired removal of the 3′-terminal intron but had no effect on removal of the upstream intron(s) in nuclear extracts.

RT-PCR and a pair of primers that amplified exon 5 through exon 6 were used to determine the efficiency of intron 5 removal. Consistent with previous findings (33), the products of MT-TPI RNAs consisted of 354 and 83 bp and derived from intron 5-containing and intron 5-free RNAs, respectively (Fig. 5). Normally, intron 5-containing and intron 5-free MT-TPI RNAs comprise, respectively, 15 and 85% of nuclear MT-TPI in transfected L cells and 24 and 76% of TPI RNA in Malme-3 cells (Fig. 5; Table 3). The Δ(pA1 and pA2) and Δ(*Nco*I-*Nae*I) constructs produced levels of the two MT-TPI RNAs that were abnormally high in absolute terms but essentially normal when expressed as a percentage of nuclear MT-TPI RNA (Fig. 5; Table 3). Therefore, a reduction in the efficiency of RNA 3′-end formation results in an accumulation of intron 5-containing and intron 5-free RNAs, presumably primarily as nascent transcripts (see Discussion), but does not change the efficiency of intron 5 removal. The Δ(*Nco*I-*Nae*I)/β-Gl construct produced levels of intron 5-containing and intron 5-free RNAs that were on average 90 and 155% of normal, respectively, in absolute terms but essentially normal when expressed as a percentage of nuclear MT-TPI RNA (Fig. 5; Table 3). The level of intron 5-containing RNA of each construct was additionally assessed as a percentage of normal by amplifying intron 5 through intron 6. In no case was the level of intron 5-containing RNA found to vary by more than 15% from the level assessed by amplifying exon 5 through exon 6 (data not shown). In summary of all of these data, neither a decrease or an increase in the efficiency of MT-TPI RNA 3′-end formation is of consequence to the efficiency of intron 5 removal.

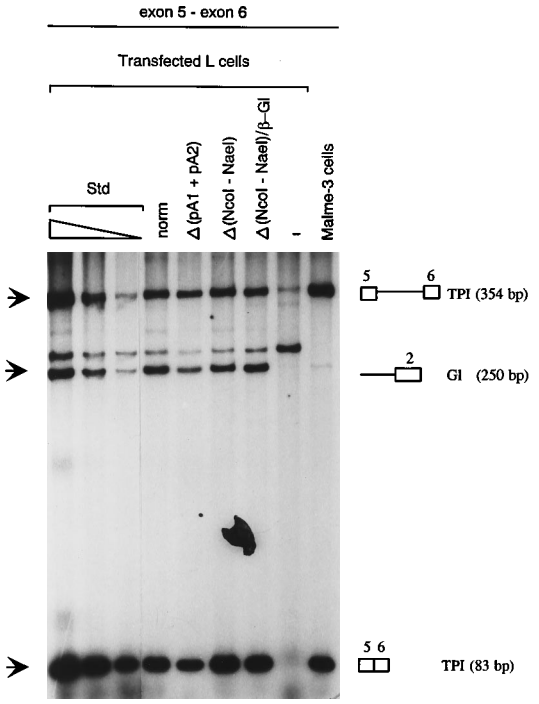

FIG. 5. The efficiency of TPI RNA 3′-end formation does not influence the efficiency with which the penultimate intron, intron 5, is removed by splicing. Nuclear RNA (2.5 μg) from L cells that were transfected with pMT-Gl DNA and the designated pMT-TPI construct was amplified by RT-PCR. TPI RNA was amplified from exon 5 through exon 6. The amplification of MT-Gl pre-mRNA, electrophoresis, and quantitation were as described in the legend to Fig. 4. The conditions used for each RT-PCR were demonstrated to be quantitative by using RNA standards (Std) that consisted of serial dilutions (1, 0.3, and 0.1 μg) of a nuclear RNA from transfected L cells. Structures and sites of the amplification products are shown at the right. The unlabeled band is a product of untransfected L-cell RNA (see Fig. 2C of reference 33). norm, normal construct.

DISCUSSION

We show here that the 3′-terminal and penultimate introns of TPI pre-mRNA are removed with efficiencies that are independent of the efficiency of RNA 3′-end formation. Mutations were generated in and around the hexanucleotide polyadenylation signals (Fig. 1) that alter the efficiency of RNA 3′-end formation, as evidenced by either an increase in the nuclear level of unprocessed 3′ ends and a concomitant decrease in the nuclear level of processed 3′ ends or a decrease in the nuclear level of unprocessed 3′ ends and a concomitant increase in the nuclear level of processed 3′ ends (Fig. 3). Each mutation was found by using RT-PCR to alter the absolute levels of nuclear RNAs that do and do not contain either

TABLE 3. Nuclear TPI RNA levels

TPI RNA	% of [(+int5[a]) + (−int5)]		% of normal	
	+int5	−int5	+int5	−int5
MT-TPI				
Normal	15 ± 5	85 ± 5	100	100
Δ(pA1+pA2)	14 ± 6	86 ± 4	131 ± 15	135 ± 38
Δ(*Nco*I-*Nae*I)	9 ± 4	91 ± 4	158 ± 60	223 ± 60
Δ(*Nco*I-*Nae*I)/β-Gl	10 ± 3	90 ± 3	90 ± 21	155 ± 11
TPI of Malme-3 cells	24 ± 5	76 ± 5		

[a] int5, intron 5.

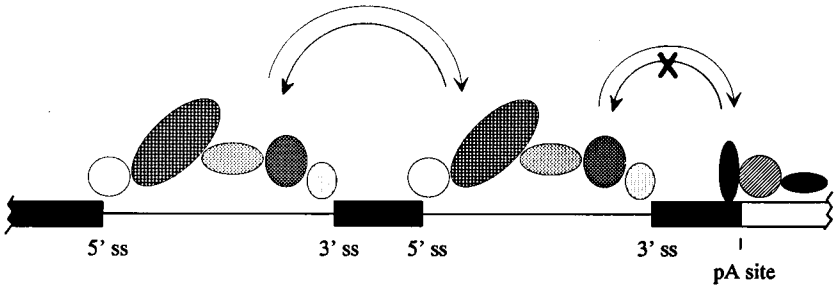

FIG. 6. A model for the interaction between factors on a nascent TPI pre-mRNA. The circles and ovals above introns (lines) represent splicing factors that minimally commit the intron to the process of splicing. The circle and ovals above exons (darkened bars) or 3′ flanking RNA (open bar) represent factors that bind at and around the site of RNA 3′-end formation (pA) and mediate the cleavage and polyadenylation reactions. Interactions between factors are specified with curved arcs that end in arrows. The X over the arc indicates that the interaction does not take place. ss, splice site.

intron 5 or intron 6 in such a way that for each intron, the ratio of intron-containing and intron-free RNAs is unchanged (Fig. 4 and 5). Mutations that alter the efficiency of 3′-end formation appear to alter the level of mRNA production primarily if not exclusively because they alter the efficiency with which nascent TPI transcripts are released from the chromatin template (Fig. 3A). There is no reason to believe that the mutations affect the efficiency with which introns 1 through 4 are removed, especially considering that the splicing of TPI pre-mRNA involves cooperativity between introns that if altered would be expected to manifest as changes in the efficiencies of intron 5 and 6 removal (33). Furthermore, none of the mutations, with the possible exception of the Δ(*Nco*I-*Nae*I)/β-Gl mutation, affects the export of nuclear mRNA to the cytoplasm, as evidenced by a near-normal ratio of nuclear and cytoplasmic mRNAs (Fig. 2).

The abnormally high level of intron-free RNA that is a consequence of inefficient RNA 3′-end formation indicates that splicing can take place on a nascent transcript, which is consistent with earlier studies of both cellular and viral RNAs (1–3, 16, 17, 22, 27), including human TPI RNA (33). Evidence that splicing can also take place on a polyadenylated RNA exists as well (12, 15, 23, 34, 35, 41). However, it is unclear whether the process of 3′-end formation can take place in an intact cell after all of the introns have been removed. The finding in studies using intact cells that only the second of two polyadenylation sites is used when the first is interrupted by an intron so as to be generated only after intron removal has been presented as evidence against the possibility that 3′-end site selection, but not necessarily 3′-end cleavage and polyadenylation, precedes intron excision (23). The issue of order cannot be addressed by simply expressing in L cells an intronless version of the TPI gene, since the complete absence of introns results in the rapid decay of nascent transcripts (33). Our previous finding for TPI pre-mRNA that the efficiency of removal of the 3′-terminal intron influences the efficiency of 3′-end formation suggests that at least the commitment to splice, if not splicing per se, is required for efficient 3′-end formation (33). Despite the fact that 3′-end formation precedes the removal of the 3′-terminal intron some of the time (33), it is tempting to speculate in view of the dependence of 3′-end formation on splicing that 3′-end formation, i.e., release of a nascent transcript from the chromatin template, without at least the commitment to splice would result in RNA decay rather than the generation of cytoplasmic mRNA. Thus, it is possible that the lack of dependence of intron removal on 3′-end formation might reflect the dead-end nature of a polyadenylated RNA that is not committed to splice. The commitment to splice appears at least in vitro to be a measurable step that involves the binding of pre-mRNA to one of several SR proteins (10). Despite the lack of an obvious role for U1 small nuclear RNP (snRNP) in the formation of the 3′ ends of cellular pre-mRNAs, in contrast to the 3′ ends of certain viral pre-mRNAs (25, 45) (see below), it might be logical to test the influence of SR proteins as well as U1 snRNP on cellular RNA 3′-end formation.

It has been shown by the Berget laboratory that mutation of the hexanucleotide polyadenylation signal of a pre-mRNA that consists of either one, two, or three introns from the adenovirus major late transcript fused upstream of the SV40 late polyadenylation sequences depresses the splicing of the 3′-terminal but not distal introns (36). The effect on the 3′-terminal intron is opposite to our finding reported here in studies using intact cells and a pre-mRNA that is identical to cellular TPI pre-mRNA with the exception of an extra 16 nt at the 5′ end (i.e., 9 nt of the MT 5′ untranslated region plus 7 nt of a synthetic linker). Differences between TPI pre-mRNA and the adenovirus-SV40 pre-RNA in the influence of 3′-end formation on splicing may reflect bona fide mechanistic differences rather than an artifact of the cell-free assay. Mechanistic differences could reflect differences between the pre-mRNAs in (i) one or more factors that mediate pre-mRNA processing, (ii) the relative rates of splicing and 3′-end formation, or (iii) the sizes of the final exons. It would be useful to have an analysis of the adenovirus-SV40 constructs using intact cells in order to ensure that the relative rates of intron removal and 3′-end formation are comparable in vitro and in vivo. The possibility that mechanistic differences between TPI and the adenovirus-SV40 pre-mRNAs may be attributable to differences in one or more processing factors is raised by the finding that U1 snRNP may coordinate the splicing and 3′-end formation of certain viral RNAs, including SV40 late and adenovirus L3 pre-mRNAs (25, 45). As alluded to above, similar findings do not exist for cellular pre-mRNAs. With regard to the second possibility, existing data do not allow for a comparison of TPI and the adenovirus-SV40 pre-mRNAs in terms of the relative strengths of the splice and 3′-end formation sites. For neither pre-mRNA did the strengths preclude the stimulation of RNA 3′-end formation by the presence of an upstream intron (32, 33, 38). The order of 3′-terminal intron removal and 3′-end formation is not fixed for TPI pre-mRNA, and it is difficult for technical reasons to determine which reaction usually takes place first (33). Polyadenylation rather than splicing is the preferred first processing reaction of the adenovirus-SV40 pre-mRNAs (35). Possibly, the step of splicing per se (which is subsequent to the commitment to splice) was sufficiently slow in the case of the adenovirus-SV40 pre-mRNAs so as to allow for the stimulation of splicing by the process of RNA 3′-end

formation. The third possibility considers that the size of the final exon of TPI pre-mRNA (565 nt) is appreciably larger than the size of the final exon of the adenovirus-SV40 pre-mRNA (125 nt). Conceivably, the distance between cleavage and polyadenylation factors bound at and around the site of 3′-end formation and splicing factors bound at and around the 3′-terminal intron is sufficiently small in the case of the viral pre-mRNA to allow for an interaction across the 3′-terminal exon so that the process of 3′-end formation can influence the process of splicing. In contrast, the size of the 3′-terminal exon of TPI pre-mRNA may be too large for such an interaction. This possibility is not readily testable with TPI pre-mRNA, since all of the deletions that decreased the size of the final exon to 450 nt or less reduced the level of product mRNA to <1% of normal (6). Notably, this possibility does not apply to the mechanism(s) by which splicing factors stimulate polyadenylation of, e.g., the 19S and 16S classes of SV40 late pre-mRNAs, which have 3′-terminal exons that are 2,116 and 1,211 nt, respectively (25, 45).

We conclude for TPI pre-mRNA, the only pre-mRNA to be tested in intact cells for bidirectional cooperativity between splicing and 3′-end formation, that the efficiency of splicing influences the efficiency of 3′-end formation but not vice versa (Fig. 6).

ACKNOWLEDGMENTS

We thank John Yates for helpful discussions and Nancy Frame for typing.

This work was supported by Public Health Service research grant DK 33938 from the National Institutes of Health and by the Council for Tobacco Research-USA, Inc. grant 3341M.

REFERENCES

1. **Aebi, M., and C. Weissman.** 1987. Precision and orderliness in splicing. Trends Genet. **3:**102–107.
2. **Baurén, G., and L. Wieslander.** 1994. Splicing of Balbiani ring 1 gene pre-mRNA occurs simultaneously with transcription. Cell **76:**183–192.
3. **Beyer, A. L., and Y. N. Osheim.** 1988. Splice site selection, rate of splicing, and alternative splicing on nascent transcripts. Gene Dev. **2:**754–762.
4. **Cheng, J., M. Fogel-Petrovic, and L. E. Maquat.** 1990. Translation to near the distal end of the penultimate exon is required for normal levels of spliced triosephosphate isomerase mRNA. Mol. Cell. Biol. **10:**5215–5225.
5. **Cheng, J., and L. E. Maquat.** 1993. Nonsense codons can reduce the abundance of nuclear mRNA without affecting the abundance of pre-mRNA or the half-life of cytoplasmic mRNA. Mol. Cell. Biol. **13:**1892–1902.
6. **Cheng, J., and L. E. Maquat.** Unpublished data
7. **Chiou, H. C., C. Dabrowski, and J. C. Alwine.** 1991. Simian virus 40 late mRNA leader sequences involved in augmenting mRNA accumulation via multiple mechanisms, including increased polyadenylation efficiency. J. Virol. **65:**6677–6685.
8. **Eckner, R., W. Ellmeier, and M. L. Birnstiel.** 1991. Mature mRNA 3′ end formation stimulates RNA export from the nucleus. EMBO J. **10:**3513–3522.
9. **Edwalds-Gilbert, G., J. Prescott, and E. Falck-Pedersen.** 1993. 3′ RNA processing efficiency plays a primary role in generating termination-competent RNA polymerase II elongation complexes. Mol. Cell. Biol. **13:**3472–3480.
10. **Fu, Y. D.** 1993. Specific commitment of different pre-mRNAs to splicing by single SR proteins. Nature (London) **365:**82–85.
11. **Green, M. R.** 1991. Biochemical mechanisms of constitutive and regulated pre-mRNA splicing. Annu. Rev. Cell Biol. **7:**559–599.
12. **Gudas, J. M., G. B. Knight, and A. B. Pardee.** 1990. Ordered splicing of thymidine kinase pre-mRNA during the S phase of the cell cycle. Mol. Cell. Biol. **10:**5591–5595.
13. **Guthrie, C.** 1991. Messenger RNA splicing in yeast: clues to why the spliceosome is a ribonucleoprotein. Science **253:**157–163.
14. **Huang, M. T.-F., and C. M. Gorman.** 1990. Intervening sequences increase efficiency and accumulation of cytoplasmic RNA. Nucleic Acids Res. **18:**937–947.
15. **Kedes, D. H., and J. A. Steitz.** 1988. Correct *in vivo* splicing of the mouse immunoglobulin κ light-chain pre-mRNA is dependent on 5′ splice site position even in the absence of transcription. Genes Dev. **2:**1448–1459.
16. **Keohavong, P., R. Gattoni, J. M. LeMoullec, M. Jacob, and J. Stévenin.** 1982. The orderly splicing of the first three leaders of the adenovirus-2 major late transcript. Nucleic Acids Res. **10:**1215–1229.
17. **Kessler, O., Y. Jiang, and L. A. Chasin.** 1993. Order of intron removal during splicing of endogenous adenine phosphoribosyltransferase and dihydrofolate reductase pre-mRNA. Mol. Cell. Biol. **13:**6211–6222.
18. **Konkel, D. A., J. V. Maizel, Jr., and P. Leder.** 1979. The evolution and sequence comparison of two recently diverged mouse chromosomal β-globin genes. Cell **18:**865–873.
19. **Krainer, A. R., T. Maniatis, B. Ruskin, and M. R. Green.** 1984. Normal and mutant human beta globin pre-mRNAs are faithfully and efficiently spliced *in vitro*. Cell **36:**993–1005.
20. **Kunkel, T. A., J. D. Roberts, and R. A. Zakour.** 1987. Rapid and efficient site-specific mutagenesis without phenotype selection. Methods Enzymol. **154:**376–382.
21. **Legrain, P., and M. Rosbash.** 1989. Some *cis* and *trans*-acting mutants for splicing target pre-mRNA to the cytoplasm. Cell **57:**573–583.
22. **LeMaire, M. F., and C. S. Thummel.** 1990. Splicing precedes polyadenylation during *Drosophila* E74A transcription. Mol. Cell. Biol. **10:**6059–6063.
23. **Liu, X., and J. E. Mertz.** 1993. Polyadenylation site selection cannot occur *in vivo* after excision of the 3′-terminal intron. Nucleic Acids Res. **21:**5256–5263.
24. **Luo, Y., and G. G. Carmichael.** 1991. Splice site choice in a complex transcription unit containing multiple inefficient polyadenylation signals. Mol. Cell. Biol. **11:**5291–5300.
25. **Lutz, C., and J. C. Alwine.** 1994. Direct interaction of the U1 snRNP-A1 protein with the upstream efficiency element of the SV40 late polyadenylation signal. Genes Dev. **8:**576–586.
26. **Maquat, L. E., R. Chilcote, and P. M. Ryan.** 1985. Human triosephosphate isomerase cDNA and protein structure: studies of triosephosphate isomerase deficiency in man. J. Biol. Chem. **260:**3748–3753.
27. **Mariman, E. C., R. J. van Beek-Reinders, and W. J. Venrooji.** 1983. Alternative splicing pathways exist in the formation of adenovirus late messenger RNAs. J. Mol. Biol. **163:**239–256.
28. **Miller, J. T., and C. M. Stoltzfus.** 1992. Two distant upstream regions containing *cis*-acting signals regulating splicing facilitate 3′-end processing of avian sarcoma virus RNA. J. Virol. **66:**4242–4251.
29. **Moore, C. L., and P. A. Sharp.** 1984. Site-specific polyadenylation in a cell-free reaction. Cell **36:**581–591.
30. **Moore, C. L., and P. A. Sharp.** 1985. Accurate cleavage and polyadenylation of exogenous RNA substrate. Cell **41:**845–855.
31. **Moore, M. J., C. C. Query, and P. A. Sharp.** 1993. Splicing of precursors to mRNA by the spliceosome, p. 303–358. *In* R. F. Gesteland and J. F. Atkins (ed.), The RNA world. Cold Spring Harbor Laboratory Press, Cold Spring Harbor, N.Y.
32. **Nesic, D., J. Cheng, and L. E. Maquat.** 1993. Sequences within the last intron function in RNA 3′ end formation in cultured cells. Mol. Cell. Biol. **13:**3359–3369.
33. **Nesic, D., and L. E. Maquat.** 1994. Upstream introns influence the efficiency of final intron removal and RNA 3′ end formation. Genes Dev. **8:**363–375.
34. **Nevins, J. R., and J. E. Darnell, Jr.** 1978. Steps in the processing of Ad2 mRNA: poly(A)$^+$ nuclear sequences are conserved and poly(A) addition precedes splicing. Cell **15:**1477–1493.
35. **Niwa, M., and S. M. Berget.** 1991. Polyadenylation precedes splicing *in vitro*. Gene Expression **1:**5–14.
36. **Niwa, M., and S. M. Berget.** 1991. Mutation of the AAUAAA polyadenylation signal depresses *in vitro* splicing of proximal but not distal introns. Genes Dev. **5:**2086–2095.
37. **Niwa, M., C. C. MacDonald, and S. M. Berget.** 1992. Are vertebrate exons scanned during splice-site selection? Nature (London) **360:**277–280.
38. **Niwa, M., S. D. Rose, and S. M. Berget.** 1990. *In vitro* polyadenylation is stimulated by the presence of an upstream intron. Genes Dev. **4:**1552–1559.
39. **Shatkin, A.** 1987. mRNA caps—old and newer hats. Bioessays **7:**275–277.
40. **Sheets, M., S. C. Ogg, and M. P. Wickens.** 1990. Point mutations in AAUAAA and the poly(A) addition site: effects on the accuracy and efficiency of cleavage and polyadenylation *in vitro*. Nucleic Acids Res. **18:**5799–5805.
41. **Tsai, M.-J., A. C. Ting, J. L. Nordstorm, W. Zimmer, and B. W. O'Malley.** 1980. Processing of high molecular weight ovalbumin and ovomucoid precursor RNAs to messenger RNA. Cell **22:**219–230.
42. **Villarreal, L. P., and R. T. White.** 1983. A splice junction deletion deficient in the transport of RNA does not polyadenylate nuclear RNA. Mol. Cell. Biol. **3:**1381–1388.
43. **Wahle, E., and W. Keller.** 1992. The biochemistry of 3′-end cleavage and polyadenylation of messenger RNA precursors. Annu. Rev. Biochem. **61:**419–440.
44. **Wassarman, D. A., and J. A. Steitz.** 1992. Interactions of small nuclear RNA's with precursor messenger RNA during *in vitro* splicing. Science **257:**1918–1925.
45. **Wassarman, K. M., and J. A. Steitz.** 1993. Association with terminal exons in pre-mRNAs: a new role for the U1 snRNP? Genes Dev. **7:**647–659.
46. **Wickens, M.** 1990. How the messenger got its tail: addition of poly(A) in the nucleus. Trends Biochem. Sci. **15:**277–281.